Received: 8 December 2019 | Accepted: 29 January 2020

DOI: 10.1111/jth.14755

ORIGINAL ARTICLE

# The development and characterization of a long acting anti-thrombotic von Willebrand factor (VWF) aptamer

Shuhao Zhu[1] | James C. Gilbert[1] | Paul Hatala[2] | Warren Harvey[3] | Zicai Liang[4] | Shan Gao[4] | Daiwu Kang[4] | Bernd Jilma[5]

[1]Guardian Therapeutics Inc, Lexington, Massachusetts, USA

[2]pHatala Consulting, Medford, Massachusetts, USA

[3]ICON Clinical Research, Dublin, Ireland

[4]Suzhou Ribo Life Science Co., Ltd, Kunshan City, China

[5]Department of Clinical Pharmacology, Medical University of Vienna, Vienna, Austria

**Correspondence**
Bernd Jilma, Department of Clinical Pharmacology, Medical University of Vienna, Waehringer Gürtel 18-20, Vienna 1090, Austria.
Email: bernd.jilma@meduniwien.ac.at

**Funding information**
These studies were funded by Guardian Therapeutics.

## Abstract

**Background:** Thrombus formation involves coagulation proteins and platelets. The latter, referred to as platelet-mediated thrombogenesis, is predominant in arterial circulation. Platelet thrombogenesis follows vascular injury when extracellular von Willebrand factor (VWF) binds via its A3 domain to exposed collagen, and the free VWF A1 domain binds to platelet glycoprotein Ib (GPIb).

**Objectives:** To characterize the antiplatelet/antithrombotic activity of the pegylated VWF antagonist aptamer BT200 and identify the aptamer VWF binding site.

**Methods:** BT100 is an optimized aptamer synthesized by solid-phase chemistry and pegylated (BT200) by standard conjugation chemistry. The affinity of BT200 for purified human VWF was evaluated as was VWF inhibition in monkey and human plasma. Efficacy of BT200 was assessed in the monkey $FeCl_3$ femoral artery thrombosis model.

**Results:** BT200 bound human VWF at an $EC_{50}$ of 5.0 nmol/L and inhibited VWF A1 domain activity in monkey and human plasma with mean $IC_{50}$ values of 183 and 70 nmol/L. BT200 administration to cynomolgus monkeys caused a time-dependent and dose-dependent effect on VWF A1 domain activity and inhibited platelet function as measured by collagen adenosine diphosphate closure time in the platelet function analyzer. BT200 demonstrated a bioavailability of ≥77% and exhibited a half-life of >100 hours after subcutaneous injection. The treatment effectively prevented arterial occlusion in an $FeCl_3$-induced thrombosis model in monkeys.

**Conclusions:** BT200 has shown promising inhibition of human VWF in vitro and prevented arterial occlusion in non-human primates. These data including a long half-life after subcutaneous injections provide a strong rationale for ongoing clinical development of BT200.

KEYWORDS

aptamers, arterial thrombosis, platelets, primates, von Willebrand factor

Manuscript handled by: David Lillicrap

Final decision: David Lillicrap, 29 January 2020

Presentation of prior abstract publication/presentation: None.

## 1 | INTRODUCTION

von Willebrand factor (VWF) is essential for the first step in maintaining hemostasis, ie, arresting hemorrhage at sites where there has been a break in the integrity of the vasculature.[1] VWF makes a molecular bridge between the collagen structural matrix that underlies the vascular endothelium and circulating blood platelets,[2] enabling platelets to adhere to sites of vessel damage and initiate formation of thrombus in order to arrest hemorrhage.[3] In addition to its role in maintaining hemostasis, VWF plays a role in shear-dependent thrombogenesis,[4] which can occur in stenotic coronary arteries or ruptured atherosclerotic plaque lesions.[3,5] An exaggerated platelet aggregation response at sites of vascular damage or artherosclerotic plaque rupture can lead to the development of vascular occlusive thrombi.[6] Animal models in mice, pigs, and dogs have shown that VWF deficiency protects against occlusive arterial thrombi.[6,7] Thrombus development in the coronary and cerebral arteries is the most common cause of mortality and morbidity, worldwide,[8] precipitating myocardial infarction or ischemic stroke, respectively. In fact, atherosclerotic lesions causing myocardial infarction or stroke may be ideal targets for VWF inhibitors.[6,9-12]

Recently, a VWF inhibitor has been authorized for acquired thrombotic thrombocytopenic purpura,[13,14] a rare disease which is complicated by microthrombotic[15,16] or more rarely by even fatal macrothrombotic events such as myocardial[17,18] or cerebral infarction.[14] This could encourage broader development of VWF inhibitors against arterial thrombosis. In this study, we characterized the anti-VWF aptamer BT200 using purified human VWF and plasma from both cynomolgus monkeys and humans. The influence of BT200 on VWF-platelet interaction was evaluated in vitro using human and cynomolgus monkey whole blood and in vivo following intravenous and subcutaneous administration to monkeys. In addition, the effect of BT200 on thrombus formation was evaluated in a femoral artery thrombosis model.

**Essentials**

- BT200 is a pegylated aptamer that inhibits von Willebrand factor (VWF) binding to platelet GPIb.
- BT200 was tested in vitro using human VWF and in cynomolgus monkeys in a Folts model.
- BT200 potently inhibited human VWF and thrombotic arterial occlusion in monkeys.
- The long half-life after subcutaneous injection further supports ongoing clinical development.

## 2 | METHODS

### 2.1 | Discovery of BT100

ARC15105 is a second-generation VWF inhibition aptamer with fully 2′OME modified chemistry that demonstrated inhibition of shear-induced platelet plug formation with a prolonged a half-life.[19] With a very short five base-pair in a typical stem-loop structure, ARC15105 is not stable especially at elevated temperature at 37°C. In order to increase the structural stability, four more extra base-pairs were added to generate BT100 with improved potency (patent #WO/2018/213697).

### 2.2 | Oligonucleotide synthesis and polyethylene gylcol conjugation

BT100, the unpegylated free nucleotide, was synthesized on an ÄKTA Oligopilot (Amersham Pharmacia Biotech) using standard phosphoramidite solid-phase chemistry. All phosphoramidites were acquired from Hongene Biotechnology Limited. BT-100 was synthesized with a free amine group attached to the 5′-end through a six-carbon linker. Purified BT-100 was then mixed with N-hydroxysuccinimide (NHS)-activated branched 40K-PEG (catalog number Y-NHS-40K; JenKem Technology USA, Inc.) at a molar ratio of BT-100 to NHS-activated branched 40K-PEG of 1:2. The reaction proceeded overnight at room temperature. The resultant was purified through anion-exchange and ultrafiltration to remove unconjugated 40K-PEG and BT-100, and BT-200, the 40K-PEG form, was obtained (Figure 1).

### 2.3 | Cocrystallization of BT100 with VWF A1 domain

The VWF A1 domain has been previously purified and cocrystallized with a DNA aptamer ARC1172.[20] Similar protein purification, crystallization, and data collection method was used. The diffraction data on the crystal of VWF A1/BT-100 RNA was collected at SSRF beam line 17U1 and processed to 2.09 Angstrom resolution in space group P21212 using XDS. A heterodimer was located in the asymmetric unit when using Phaser as a molecular replacement program with search model PDB ID 1SQ0. After the initial refinement using program Refmac5, the density of RNA was observed. Then, cycles of model building using Coot and refinement was iterated to complete the final structure of VWF A1/BT-100 aptamer RNA.

### 2.4 | In vitro binding of BT200 to purified human VWF

The affinity of BT200 for purified human VWF was evaluated using an enzyme-linked immunosorbent assay (ELISA) method. In this study, purified human VWF protein (Sino Biological; Catalog Number 10973-H08c) was dissolved in Dulbecco's phosphate buffered saline (dPBS) buffer at 10 µg/mL and 100 µL of this solution was added to each well of a Nunc Maxisorp 96-well plate (Nunc™ 446612). The plate was incubated overnight at 4°C. The plate was then washed and blocked by 5% bovine serum albumin (BSA) in dPBS at room temperature for 90 minutes. The blocked

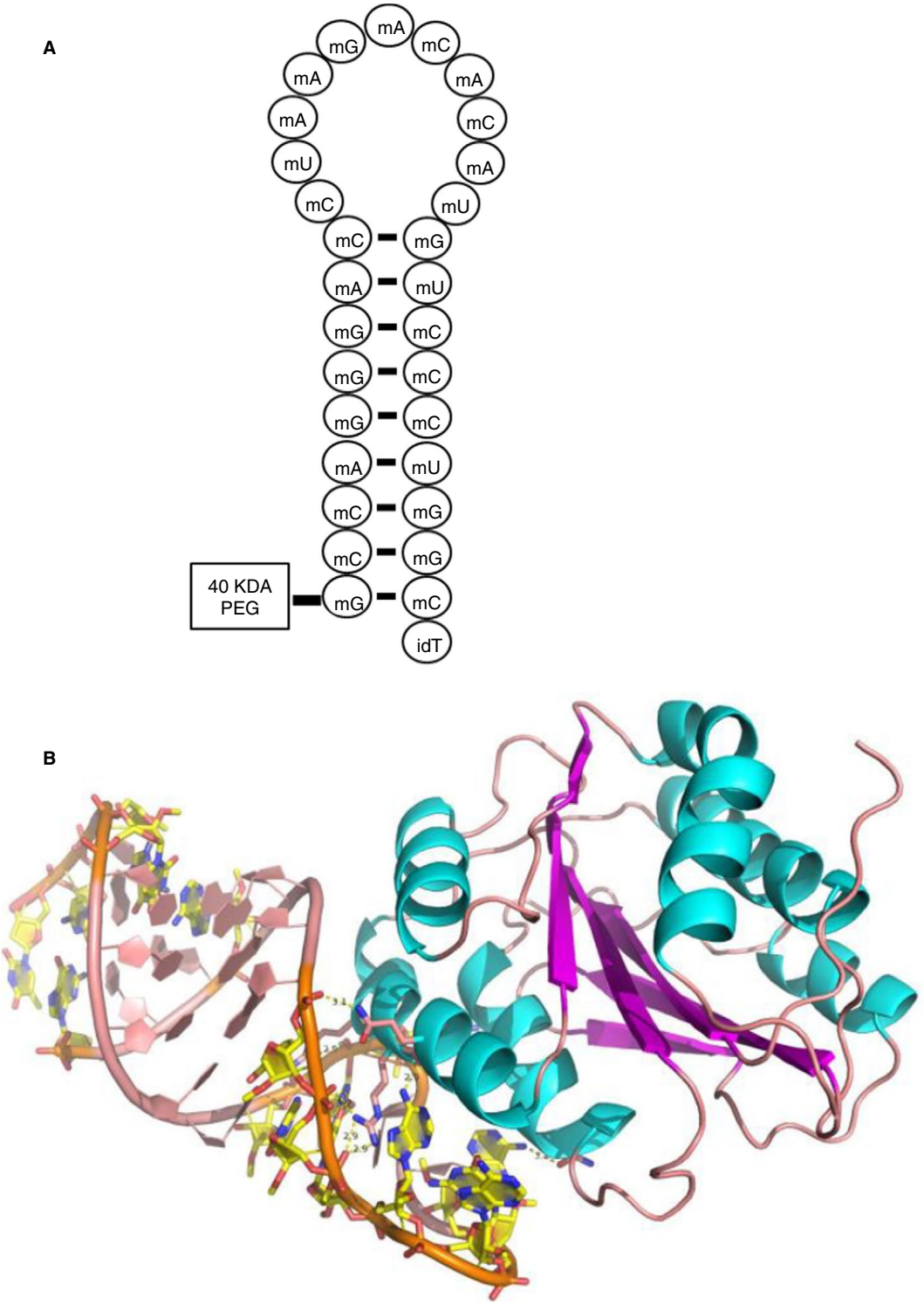


**FIGURE 1** A, Secondary structure of the anti von Willebrand factor aptamer BT200. The letter "m" stands for methylated and the letters ACGU for the nucleobases adenine, cytosine, guanine, and uracil. B, Cocrystal structure of the unpegylated aptamer BT100 with the von Willebrand factor A1 domain

plate was then washed and serially diluted BT200 concentrations were added into the plate and incubated at 37°C for 2 hours. Following washing, 100 µL of recombinant rabbit monoclonal anti-polyethylene glycol antibody (PEG-B-47 [from Abcam #ab51257]) at 1 µg/mL in 1% BSA/dPBS was added to each well and incubated for 1 hour at room temperature. The washed plate then had 100 µL of horseradish peroxidise (HRP) linked goat anti-rabbit (Cell Signaling Technology, Catalog Number 7074) in dPBS with 1% BSA added to each well for 60 minutes at room temperature. To detect HRP, 100 µL of Slow TMB solution was added to each

well and incubated at room temperature for 30 minutes. To stop the reaction, 100 µL of 2 N $H_2SO_4$ was added to each well and the plate was then read at 450 nm for absorbance and the mean absorbance under each set of conditions was recorded.

### 2.5 | In vitro inhibition of antibody binding to the VWF A1 domain in cynomolgus monkey and human plasma

Whole blood was drawn from three cynomolgus monkeys into blood collection tubes containing 3.2% sodium citrate (9:1) and plasma was separated by centrifugation at 1800 *g*. A BT200 stock solution of 1 mg/mL in PBS was diluted into plasma to final concentrations of 1, 3, 10, 30, 100, 300 nmol/L, and 1 and 3 µmol/L.

Citrated human plasma was acquired from Jiangsu Provincial Institute of Hematology, which provides non-O plasma for normal human sample mixing. A 10 mg/mL (1 mmol/L) BT200 stock solution in 0.85% NaCl was diluted into plasma samples to final concentrations of 1, 3, 10, 100, 300 nmol/L, and 1 µmol/L.

The REAADS® VWF Activity Test Kit (Corgenix, Catalog Number 10826) was utilized to measure the effects of BT200 on functional VWF in these monkey and human plasma samples. A monoclonal antibody specific for the portion of VWF, which binds platelets, is coated to the 96-microwell plates.[21,22] Diluted plasma samples are incubated in the wells, which are washed and bound antigen is detected by a horseradish peroxidase conjugated anti-human VWF detection antibody.

Analysis of VWF activity was performed according to manufacturer's instructions. VWF activity in relative percent concentration is determined against a curve made from the reference plasma provided with the kit. For each incubation condition, VWF activity was reported in percent (%) of normal, relative to a calibrator that has been standardized against the third International Standard for factor VIII and VWF in plasma. This activity was then plotted against BT200 concentration to determine the concentration resulting in 50% inhibition ($IC_{50}$) values.

### 2.6 | Determination of VWF ristocetin cofactor activity (RCo) and Gp1b binding activity

VWF:RCo (BC von Willebrand reagent [Siemens]) and VWF glycoprotein Ib (GpIb) binding activity (Innovance, Siemens) were determined by commercially available assays as described previously.[23,24]

### 2.7 | Inhibition of VWF-platelet binding activity in cynomolgus monkeys following intravenous and subcutaneous administration

Inhibition of VWF-platelet binding activity was evaluated following intravenous (IV) and subcutaneous (SC) injection of BT200 to cynomolgus monkeys as bolus doses in 0.9% saline. Three 3- to 5-year-old male cynomolgus monkeys (Guangzhou Aojun Biotech Ltd.) with body weights ranging from 3.5 to 5 kg were used. One monkey was infused BT200 IV at a dose of 3 mg/kg and two additional monkeys received BT200 SC at doses of 1 and 3 mg/kg, respectively. Citrated blood was drawn prior to dosing and at 1, 4, 8, 24, 48, 96, 168, 240, and 336 hours post-administration and analyzed using the REAADS® VWF Activity Test Kit.

### 2.8 | Effect of BT200 on VWF-dependent platelet plug formation in cynomolgus monkey and human whole blood

Sixteen cynomolgus monkeys (2.6-3.9 kg, 3-5 years of age) were obtained from Xishan Zhongke Laboratory Animal Co. Human blood was collected from 14 healthy volunteers (seven males, seven females) with ages ranging from 25 to 60 years and different blood types (A [4], B [3], AB [3], O [4]).

Samples were prepared from whole blood drawn into citrated (0.32%) blood collection tubes. BT200 stock solutions in 0.9% NaCl were added to citrated blood samples to final concentrations of 1, 10, 40, 60, 80, 100 and 300 nmol/L; and 1 µmol/L in monkey samples and 0.1, 0.3, 1, 3, 6, 10, 20, 30, 100, 300 nmol/L; 1 and 3 µmol/L in human samples. After incubation at 37°C for 15 minutes, platelet plug formation was measured by collagen/adenosine diphosphate-induced closure time (CADP-CT) with a platelet function analyzer, PFA-200 (Siemens). Normal saline was used as a negative control. Maximal CT measured by the PFA 200 is 5 minutes and the instrument gives a result of >300 seconds if this time is exceeded.

### 2.9 | Pharmacokinetics of BT200 in cynomolgus monkeys

In a single-dose pharmacokinetics (PK) study in cynomolgus monkey, BT200 was injected SC at single doses of 0.5, 2, 10 mg/kg (three monkeys per sex and dose group). In addition, BT200 was infused IV at a single dose of 2 mg/kg (three monkeys per sex and dose group) to investigate the bioavailability of BT200.

### 2.10 | Effect of BT200 on $FeCl_3$-induced femoral artery thrombosis

The effects of three different single doses of BT200 and a reference drug, tirofiban hydrochloride (a GPIIbIIIa inhibitor), on thrombus formation and bleeding time were evaluated in a $FeCl_3$-induced thrombosis model[25] in femoral arteries of cynomolgus monkeys. Fifteen male cynomolgus monkeys (Guangxi Guidong Primate Development Experiment Co., Ltd.) weighing between 2.9 and 4.3 kg and aged 3 to 5 years were used for the experiments. In the initial experiment,

the animals were randomly divided into three groups (N = 5/group) according to body weight and treated either subcutaneously with vehicle (phosphate buffered saline) or BT200 (1 mg/kg) or intravenously with tirofiban hydrochloride (0.06 mg/kg, Lunanbeite Pharmaceutical Co., Ltd.). After the first experiment, 10 animals were assigned to a 4-week washout period and then regrouped into two groups (N = 5/group) and treated subcutaneously with BT200 at 50 or 100 μg/kg.

Animals receiving vehicle or BT200 were dosed at 24 hours prior to $FeCl_3$ treatment while animals receiving tirofiban hydrochloride were dosed 1 hour before $FeCl_3$ treatment. One hour before $FeCl_3$ thrombus induction, each animal received intramuscular injection of 1.5 mg/kg Zoletil followed by induction of anesthesia with 2% to 3% isoflurane with an oxygen exchange rate of 2 L/min. Once animals were fully anesthetized, 1.5% isoflurane was used for maintenance. The experimental animals were placed on a constant-temperature warming plate to maintain a constant body temperature. Blood pressure, heart rate, and body temperature were monitored throughout the procedure. A blunt instrument was used to expose approximately 2 to 3 cm of the left femoral artery, and the exposed blood vessel was covered with gauze soaked in (37°C) normal saline, to maintain moisture and protect the tissue at the site of vascular separation. A Doppler probe was placed on the exposed left femoral artery. Before placement, the probe was filled with acoustic coupling gel to prevent air bubbles in the gel. The probe was placed perpendicular to the blood vessel. Blood flow was continuously monitored and recorded.

Prior to $FeCl_3$ treatment, blood flow was monitored for a minimum of 5 minutes; this record served as the baseline blood flow. Two sheets of filter paper (3 × 5 mm) were soaked with 40% $FeCl_3$ solution and externally applied to the surface of the vascular adventitia upstream of the probe for 10 minutes, one at the anterior arterial wall and one at the posterior arterial wall. After removing the filter paper, a cotton swab soaked in normal saline was used to swab the wound, to clear away any residual $FeCl_3$ and keep the blood vessel moist. Measurement of blood flow continued for 60 minutes or until the blood flow was completely occluded (a blood flow rate of 0). During this process, the two parameters reflecting thrombus formation time were: (a) timing from the beginning of $FeCl_3$ treatment to when the blood flow rate dropped to 20% or less of the baseline blood flow rate, and (b) time when the blood flow was completely occluded, ie, the blood flow rate was 0.

Bleeding time was measured before infusion (−24 hours) and 24 hours after infusion (0 hour) in the vehicle and BT200 treated groups. In the tirofiban group, bleeding time was measured before infusion (−1 hour) and 1 hour after infusion (0 hour). The skin on the ventral side of the experiment animal's upper limb was prepared with Anerdian disinfection. Keeping the skin suitably taut and avoiding visible areas of superficial vein distribution, a bleeding time device was placed against the skin and a longitudinal incision (1 cm long, 1 mm wide, and 5 mm deep) was made. Following the incision, sterile filter paper was lightly touched to the surface of the wound every 15 seconds, until the filter paper showed no obvious traces of blood. The time to no obvious traces of blood was recorded as the bleeding time.

In addition to measuring the effects on blood flow and bleeding time, the effects of BT200 on VWF activity (measured using REAADS®), CADP-CT (measured using the PFA 200), and ADP-induced platelet aggregation were evaluated. These effects were measured in blood samples taken at −24 hours (baseline value), −18 hours (intermediate value), 0 hour (peak), and 1.5 hours following $FeCl_3$ treatment for the vehicle control and BT200-treated animals. Blood samples were also collected for BT200-treated animals at −24, −18, 0, and 1.5 hours following $FeCl_3$ infusion for the determination of plasma BT200 concentrations using a high-performance liquid chromatography-ultraviolet (HPLC-UV) method with a lower limit of quantitation of 0.5 μg/mL.

### 2.11 | Statistical analysis

Data are presented as mean and standard deviations or standard error of the mean. For reasons of statistical robustness, non-parametric analyses were used where *P* values are indicated. A Friedman analysis of variance (ANOVA) followed by Wilcoxon test was used for paired samples, and a Kruskal-Wallis ANOVA followed by *U* test for unpaired samples. A $P < .05$ was considered significant and a Bonferroni correction applies to multiple comparisons (eg, tirofiban and BT200 vs control), but *P*-value corrections were not performed for post-hoc tests in which the ANOVA was highly significant and concentration- and/or time-dependent effects were tested.

## 3 | RESULTS

### 3.1 | Cocrystallization of BT100 with vWF A1 domain

Multiple nucleotides of BT-100 directly interacted with amino acid residues of the recombinant VWF A1 domain, and mostly these nucleotides reside in the loop, suggesting that the loop sequences provided the VWF A1 domain binding interaction while the stem sequences provided the aptamer structural stability. For example, ARG632 provides interaction with 19 mA and 20 mU and ARG636 provides multiple contacts with 10 mC, 11 mU, and 12 mA. Additionally, 9 mC interacts with GLN639 and 15 mA interacts with GLN604. Very similar to ARC1172, BT100 occupies mostly the botrocetin binding surface on the VWF A1 domain.[20]

### 3.2 | BT200 binds to purified human VWF with high affinity

BT200 binding to purified human VWF protein was evaluated at concentrations ranging from 0.03 to 1000 nmol/L. BT200 bound to purified human VWF in a concentration-dependent manner (Figure 2).

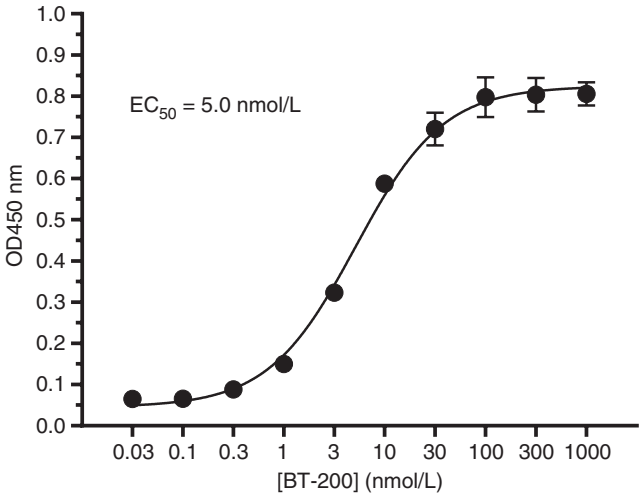


**FIGURE 2** Binding of BT200 to purified human von Willebrand factor. EC50, Concentration resulting in 50% maximal effect; nmol/L, nanomolar; OD, optical density; data are presented as mean absorbance ± SD for each concentration (N = 6/concentration)

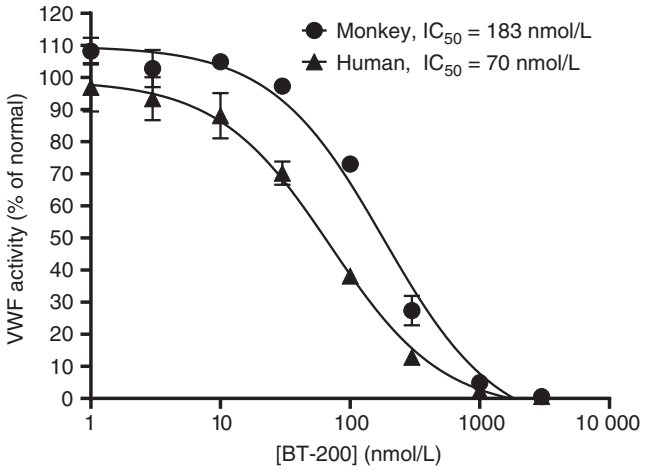


**FIGURE 3** Effect of BT200 on von Willebrand factor (VWF) A1 domain activity in cynomolgus monkey and human plasma as measured using the REAADS® activity assay. VWF A1 domain activity is presented as relative percent concentration, which was determined against a curve made from the reference plasma provided with the kit

The mean concentration resulting in 50% maximal absorbance ($EC_{50}$) in three independent experiments was 5.0 nmol/L (51 ng/mL) with a coefficient of variation (CV) value of 11%. The results of this in vitro binding study demonstrate that BT200 binds to VWF with high affinity.

### 3.3 | BT200 inhibits VWF-platelet binding activity in plasma from cynomolgus monkeys and humans

BT200 caused a concentration-dependent inhibition of VWF A1 domain activity in cynomolgus monkey plasma measured as inhibition of the REAADS® assay A1 antibody binding. A mean $IC_{50}$ value for the three monkeys of 183 nmol/L was measured (Figure 3). As in monkeys, BT200 caused a concentration-dependent inhibition of VWF A1 domain activity in human plasma (Figure 3); the $IC_{50}$ values determined in three independent experiments had an average of 70 nmol/L.

Further, BT200 concentration-dependently inhibited VWF:RCo and VWF:GpIb binding activity (Figure S1 in supporting information). The results suggest that inhibition of VWF by BT200 in both monkey and human plasma was mediated by blocking the A1 domain.

### 3.4 | BT200 inhibits VWF-platelet binding activity following intravenous and subcutaneous administration to cynomolgus monkeys

BT200 administration to monkeys caused a time-dependent and dose-dependent effect on VWF A1 domain activity (Figure 4). The effects following IV infusion appeared to peak at the 1-hour post-dose time point, and persisted for >168 hours. Following SC injection, maximum effects were seen at 8 to 24 hours post-dose and persisted for 96 hours (1 mg/kg) to >168 hours (3 mg/kg) post-dose. The magnitude and duration of the effect was similar following IV or SC administration

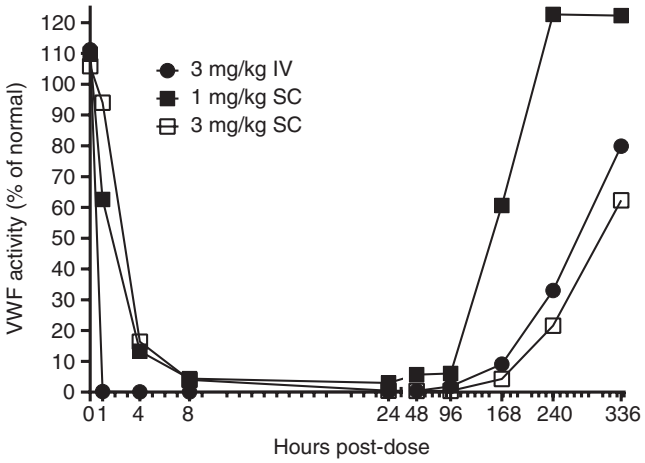


**FIGURE 4** Effect of BT200 on VWF activity in monkeys following IV and SC administration as measured using the REAADS® activity assay. VWF A1 domain activity is presented as relative percent concentration which was determined against a curve made from the reference plasma provided with the kit. IV, intravenous infusion; SC, subcutaneous injection; VWF, von Willebrand factor

of a 3 mg/kg dose. The results demonstrate a high affinity and long-lasting interaction between BT200 and the A1 domain of VWF in vivo.

### 3.5 | BT200 inhibits VWF dependent platelet plug formation in whole blood from cynomolgus monkeys and humans

BT200 inhibited platelet function under high shear rates in whole blood collected from cynomolgus monkeys, as evidenced by a

**TABLE 1** Collagen/adenosine diphosphate-induced closure time in cynomolgus monkey and human blood samples following incubation with BT200

| | Closure time (s), mean ± SD | |
|---|---|---|
| BT200 (μg/mL) | Cynomolgus monkey (N = 16) | Human (N = 14) |
| 0 | 56 ± 9 | 92.3 ± 21 |
| 0.001 | - | 101 ± 23 |
| 0.003 | - | 91.9 ± 14 |
| 0.01 | 55 ± 10 | 94.3 ± 18 |
| 0.03 | - | 102 ± 21 |
| 0.06 | - | 112 ± 31 |
| 0.1 | 59 ± 7 | 140 ± 44*** |
| 0.2 | - | 182 ± 59*** |
| 0.3 | - | 281 ± 32*** |
| 0.4 | 83 ± 25 | - |
| 0.6 | 136 ± 74*** | - |
| 0.8 | 231 ± 86*** | - |
| 1 | 289 ± 30*** | >300 ± 0*** |
| 3 | >300 ± 0*** | >300 ± 0*** |
| 10 | >300 ± 0*** | >300 ± 0*** |
| 30 | - | >300 ± 0*** |

–Concentration not tested.

***$P$ < .001.

concentration-dependent increase in CADP-CT (Table 1). Incubation with BT200 concentrations of ≥0.6 μg/mL significantly prolonged CADP-CT ($P$ < .001) when compared to vehicle control. No sex-dependent differences were seen (analysis not shown). BT200 also inhibited platelet plug formation in human whole blood in a concentration-dependent manner (Table 1). In human blood, significant prolongation of CADP-CT was seen at concentrations ≥ 0.1 μg/mL.

### 3.6 | Pharmacokinetics of BT200 in cynomolgus monkeys

The PK and ratio of exposure parameters following a single dose of BT200 are presented in Table 2. In summary, plasma exposures as measured by peak concentration ($C_{max}$), area under the concentration time curve from time 0 to the last quantifiable time point estimated using the linear log trapezoidal rule ($AUC_{last}$), and area under the concentration time curve from time 0 to infinity ($AUC_{\infty\text{-OBS}}$) were linear from 0.5 to 10 mg/kg in cynomolgus monkey. The $T_{1/2}$ was approximately 3.75 days. The average bioavailability of BT200 following SC injection calculated from the ratio of mean $AUC_{\infty\text{-OBS}}$ after 2 mg/kg was 77.5%. No significant sex differences were observed in systemic exposure of BT200 (area under the concentration versus time curve [AUC] and $C_{max}$).

**TABLE 2** Pharmacokinetic parameters (mean ± SD) of BT200 in cynomolgus monkeys after a single administration at 0.5, 2, and 10 mg/kg

| | Intravenous | Subcutaneous | | |
|---|---|---|---|---|
| PK parameter | 2 mg/kg | 0.5 mg/kg | 2 mg/kg | 10 mg/kg |
| $AUC_{\infty\text{-OBS}}$ (h·μg/mL) | 4750 ± 906 | 1080 ± 77.9 | 3680 ± 548 | 23 500 ± 746 |
| $AUC_{last}$ (h·μg/mL) | 4570 ± 896 | 924 ± 55.7 | 3490 ± 532 | 22 800 ± 768 |
| $C_0$ (μg/mL) | 61.6 ± 10.0 | ND | ND | ND |
| $Cl_{obs}$ (mL/h/kg) | 0.437 ± 0.097 | ND | ND | ND |
| $C_{max}$ (μg/mL) | ND | 7.01 ± 0.60 | 27.4 ± 2.56 | 152 ± 14.5 |
| $MRT_{last}$ (h) | 93.1 ± 16.9 | 88.7 ± 1.85 | 104 ± 22.2 | 129 ± 5.70 |
| $T_{1/2z}$ (h) | 88.2 ± 20.1[a] | 82.6 ± 10.3[b] | 83.5 ± 22.6[a] | 103 ± 3.5[c] |
| $T_{max}$ (h) | ND | 28.0 ± 3.10 | 28.0 ± 3.10 | 30.0 ± 0.00 |
| $Cl/F_{obs}$ (mL/h/kg) | ND | 0.466 ± 0.032 | 0.554 ± 0.086 | 0.426 ± 0.013 |
| $Vss_{obs}$ (mL/kg) | 46.8 ± 7.58 | ND | ND | ND |
| $Vz_{obs}$ (mL/kg) | 54.1 ± 9.94 | ND | ND | ND |
| $Vz/F_{obs}$ (mL/kg) | ND | 55.3 ± 5.90 | 65.4 ± 14.3 | 63.5 ± 3.84 |
| $F$ | 100% | 90.9%~ | 77.5% | 98.9%~ |

Abbreviations: $AUC_{\infty\text{-OBS}}$, area under the concentration versus time curve from time 0 to the last quantifiable timepoint; $AUC_{last}$, area under the first moment curve from time 0 to time of last measurable concentration; $C_0$, initial concentration at time 0 following bolus intravenous injection; $Cl/F_{obs}$, apparent total clearance of the drug from plasma after drug administration; $Cl_{obs}$, clearance of drug; $C_{max}$, maximum observed concentration; $F$, bioavailability; ~estimated after dose normalization of AUC values; $MRT_{last}$, mean residence time; ND, not determined; $T_{1/2z}$, elimination half-life; PK, pharmacokinetics; $T_{max}$, time to maximum concentration after dosing; $Vss_{obs}$, volume of distribution of drug at steady state; $Vz/F_{obs}$, apparent volume of distribution in terminal phase after drug administration; $Vz_{obs}$, volume of distribution following intravenous administration.

[a]The time intervals for calculation of $T_{1/2z}$ were 240-504 hours.

[b]The time intervals for calculation of $T_{1/2z}$ were 72-240 hours.

[c]The time intervals for calculation of $T_{1/2z}$ were 168-408 hours.

### 3.7 | BT200 inhibits thrombus formation, VWF activity, and platelet function following subcutaneous injection to cynomolgus monkeys

Subcutaneous injection of BT200 significantly prolonged the thrombus formation time in an $FeCl_3$-induced femoral artery thrombosis model in primates. Increased time to blood flow <20% of baseline and time to blood flow of 0 were seen at both 0.1 and 1 mg/kg when compared to the vehicle control-treated group (Figure 5). There was no vessel occlusion during the 60-minute observation period following injection of 1 mg/kg BT200. At a lower dose level of 0.05 mg/kg, BT200 had no significant effect on thrombus formation time. Infusion of tirofiban hydrochloride (0.06 mg/kg) prolonged the time to thrombus formation; however, the differences from the vehicle control group were not significant. BT200 decreased VWF antigen levels by 19% versus baseline, but only by 12% as compared with the control group (Figure S2 in supporting information).

Inhibition of VWF activity was also noted following infusion of BT200. Both the magnitude and duration of this inhibition were dose-dependent. At 1 mg/kg, maximum effects were seen at the first post-dose evaluation time point of 6 hours post-dose and remained consistent throughout the evaluation period. At the lower dose levels of 0.05 and 0.1 mg/kg, BT200 significantly inhibited the activity of VWF at the peak (24 hours post-dose) and 1.5 hours post $FeCl_3$ administration (25.5 hours post-dose) time points (data not shown). There were no significant differences in the activity of the VWF when compared to baseline for the vehicle control or tirofiban hydrochloride (data not shown) treated groups.

Consistent with previous in vitro results, BT200 inhibited platelet plug formation as measured by a prolongation in CADP-CT (Table 3). BT200 extended closure time at both 0.1 and 1 mg/kg and the magnitude and duration of the effect was dose-dependent. BT200 dose dependently increased bleeding time (Figure S3 in supporting information): despite a significant prolongation of bleeding time at 1 mg/kg (16.7 minutes $P = .005$ versus 2.8 minutes vehicle), no signs of bleeding occurred in any animals. There were no differences in bleeding time before and after infusion in the vehicle control or tirofiban hydrochloride treated groups.

## 4 | DISCUSSION

von Willebrand factor is an interesting target for primary or secondary prevention of cardiovascular diseases,[26] particularly in high-risk patients. Numerous epidemiologic studies have established that an excess of VWF predicts an increased risk for both stroke[9] and stroke mortality.[27] Conversely, deficiency of VWF may protect against cardiovascular disease or stroke.[28,29] For example, von Willebrand disease patients with average VWF levels of 24% had a 35% to 67% reduced risk for ischemic stroke when compared to controls, suggesting that partial inhibition of VWF could be protective in the stroke-prone population.[28] The underlying pathophysiologic mechanism of large artery atherosclerosis stroke is likely shear- and VWF dependent platelet thrombus formation in the setting of atherosclerotic stenosis.[5,6,9] Importantly, VWF and platelet rich thrombi are more resistant to thrombolysis and are associated with poorer outcome after revascularization in stroke patients.[30,31]

At one end extracellular VWF binds to exposed collagen, for example that found in ruptured plaques, via its A3 domain, and at the other end VWF uses its A1 domain to bind to platelet GPIb, thus serving as a bridge between collagen and platelets.[32] VWF, therefore, is a key player in mouse models of acute stroke.[33] Due to its binding to the A1 domain, BT200 pharmacologically blocks the bridge between collagen and platelets. This property confers a degree of anatomic specificity to the pharmacology of BT200, favoring

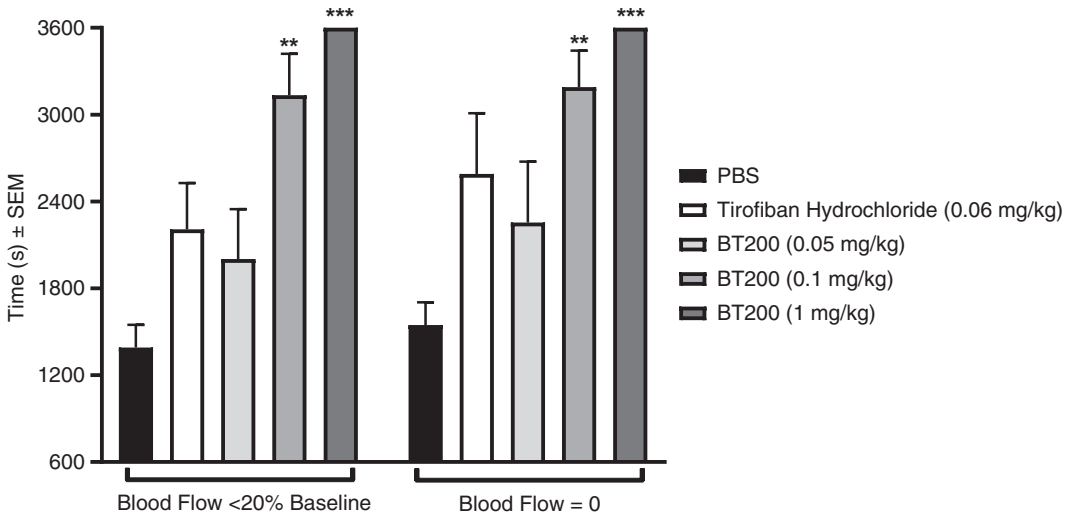


**FIGURE 5** Effect of BT200 on $FeCl_3$-induced thrombus formation time in monkeys. Time to reduction of blood flow to <20% of baseline or no blood flow. Time to thrombus formation exceeded the maximum observation period of 2 hours (3600 s) after subcutaneous injection of 1mg/kg BT200. $^{**}P = .008$, $^{***}P = .005$, Compared with PBS control (Kruskal-Walis analysis of variance followed by *U* test). SEM, standard error

**TABLE 3** Effect of BT200 on collagen/adenosine diphosphate-induced closure time following subcutaneous injection to cynomolgus monkeys

| | CADP-CT (N = 5/group)[a] | | | | | | | |
|---|---|---|---|---|---|---|---|---|
| | Vehicle control | | 0.05 mg/kg BT200 | | 0.1 mg/kg BT200 | | 1 mg/kg BT200 | |
| Hours post-dose | Mean | SEM | Mean | SEM | Mean | SEM | Mean | SEM |
| 0 | 56 | 4 | 70 | 4 | 57 | 2 | 67 | 3 |
| 6 | 61 | 2 | 76 | 6 | 74 | 8 | 300** | 2 |
| 24 | 72 | 5 | 138* | 31 | 226** | 7 | 300** | 1 |
| 25.5 | 63 | 5 | 88* | 2 | 193** | 1 | 300** | 3 |

Abbreviations: CADP-CT, collagen/adenosine diphosphate-induced closure time; CT, closure time; SEM, standard error of the mean.

[a]CADP-CT was measured using the PFA-200. Results are reported as CT in seconds. The assay has a maximum of 300 seconds.

*$P < .05$.

**$P < .01$ versus vehicle.

arterial over venous circulatory systems, and thromboembolism from arterial plaque rupture over cardioembolism from atrial fibrillation. BT200's mechanistic site of action is upstream in the cascade of platelet thrombogenesis from that of conventional platelet inhibitors of platelet activation (eg, aspirin, clopidogrel, ticagrelor) and of platelet aggregation (eg, abciximab, tirofiban), and therefore works in a complementary fashion with them.

BT200 is an agent offering an innovative approach to secondary stroke prevention with a focus on VWF. BT200 is a pegylated synthetic RNA oligonucleotide drug candidate belonging to the medicinal chemical family known as aptamers,[34] which offers the opportunity to rapidly develop a reversal agent. Based on the mechanism of action of BT200, mucosal bleeding will likely be the predominating type of bleeding, such as epistaxis observed under caplacizumab.[13] Consistent with the effect of caplacizumab in baboons, BT200 also prolonged the bleeding time in cynomolgus monkeys. This class effect was associated with increased surgical blood loss under therapeutic doses of caplacizumab (Cablivi European Assessment report). Thus, availability of a reversal agent is a desirable asset in case emergency reversal of VWF inhibition is needed.

In vivo stability of BT200 is enhanced by its methylated oligonucleotide backbone, while it is also pegylated to improve pharmacokinetics and provide a convenient subcutaneous clinical dosing schedule based on the ~3.5 day $T_{1/2}$ in non-human primates. This half-life represents a substantial improvement when compared to the 2-hour half-life of the intravenously infused ARC1779, an anti-VWF aptamer coupled to a 20 kD polyethylene (PEG) residue,[35] which successfully established proof of concept in various patient populations.[36-39] Whereas drugs conjugated with 20 kD PEG are usually filtered renally, molecules with larger PEG sizes (>30 kD) are cleared by the reticulo-endothelial system,[40] which is also true for pegylated aptamers.[34]

Despite having a similar PEG size to ARC15105,[19] the stem stabilization found in BT-200 further improved its half-life up to 103 hours after 10mg/kg compared with ARC15105 (~66 hours after 20 mg/kg) or >3-fold compared with a 8 mg/kg dose of the nanobody caplacizumab in cynomolgus monkeys.[41] However, the affinity of BT200 for VWF is in the same low nanomolar range as caplacizumab. The co-crystallography studies showed that BT200 specifically binds to the A1 domain of primate VWF and thereby inhibits VWF binding to platelet GPIb, the first step in the cascade of platelet-mediated thrombogenesis. Functional inhibition of platelet thrombogenesis by BT200 has been demonstrated by in vitro human pharmacology studies and in vivo studies in nonhuman primates described in this study. The reduction of VWF antigen levels by <20% at 24 hours after BT200 injection indicates no major effect on VWF clearance, which is in contrast to the 46% reduction induced by caplacizumab.[42] As VWF antigen levels still fell into the high normal range after BT200 injection, this minor effect is unlikely to play a major role in the effective prevention of arterial thrombosis seen in the Folts model. Preclinical testing of novel anti-platelet drugs in a monkey model is a rarity similar to use of the $FeCl_3$ model in primates. This was not only necessary due to the limited cross-reactivity of aptamers between species, but it also represents a particular strength of this study. This is because of interspecies differences in hemostasis[43] as well as other differences in important physiological variables between small rodents and larger non-rodents.[44] However, the protective effect of BT200 on arterial occlusion in primates matches the beneficial effects of VWF deficiency or blockade seen in mice, dogs, or pigs using $FeCl_3$ induced arterial occlusion.[7,45] A further strength of the monkey study was that it included both a placebo and the fibrinogen receptor inhibitor tirofiban as an active control, which was given at a dose that exceeded the loading dose in humans 2.5-fold.

## 4.1 | Limitations

While even potent platelet inhibitors like tirofiban or prasugrel do not optimally inhibit shear-dependent platelet plug formation,[46,47] we cannot exclude that expanding the limited sample size would have resulted in a significant effect of tirofiban. However, the 3R

principle (replacement, refinement, and reduction of animals in research) mandates the use of minimal sample sizes, particularly in non-human primate trials. Whereas proof of concept has previously been established for VWF inhibitors in various animal models of stroke,[6] stroke models for stroke recurrence are unfortunately lacking, as are comorbidities or atherosclerosis in rodent models.[44] However, a human trial has already provided proof of concept that VWF inhibition by ARC1779 markedly reduces the onset and numbers of microembolic signals in patients after carotid endarterectomy,[36] which are strong predictors of stroke.[48] This is encouraging, because other antiplatelet drugs including clopidogrel did not reduce the number of microembolic signals after endarterectomy.[49]

In conclusion, BT200 has shown promising inhibition of human VWF in vitro and prevented arterial occlusion in non-human primates. These data including a long half-life after subcutaneous injections provide a strong rationale for ongoing clinical development of BT200.

## ACKNOWLEDGMENTS

The authors thank Dr Paul Tarantino and Dr Robert Schaub for their editorial contributions and review of the manuscript. The authors would like to dedicate this work to Prof. Evan Sadler.[50]

## CONFLICTS OF INTEREST

SZ and JG are employees of Guardian Therapeutics, Inc, PH, WH and BJ consultants. Drs SZ, JG, and BJ also have an equity position with Guardian. SG and DW are employees and ZL is the chairman of Suzhou Ribo Life Science Co.

## AUTHOR CONTRIBUTIONS

All authors contributed to the preparation of the article and met the required conditions for authorship. All authors participated in the design, analysis, and interpretation of the data. All authors revised the article for critical content. All the authors revised the article for critical content.

## ORCID

*Bernd Jilma* https://orcid.org/0000-0001-5652-7977

## REFERENCES

1. Sadler JE. von Willebrand factor assembly and secretion. *J Thromb Haemost*. 2009;7(suppl 1):24-27.
2. Lenting PJ, Casari C, Christophe OD, Denis CV. von Willebrand factor: the old, the new and the unknown. *J Thromb Haemost*. 2012;10:2428-2437.
3. Sadler JE. Biochemistry and genetics of von Willebrand factor. *Annu Rev Biochem*. 1998;67:395-424.
4. André P, Hainaud P, Bal dit Sollier C, Garfinkel LI, Caen JP, Drouet LO. Relative involvement of GPIb/IX-vWF axis and GPIIb/IIIa in thrombus growth at high shear rates in the guinea pig. *Arterioscler Thromb Vasc Biol*. 1997;17:919-924.
5. Le Behot A, Gauberti M, Martinez De Lizarrondo S, et al. GpIbalpha-VWF blockade restores vessel patency by dissolving platelet aggregates formed under very high shear rate in mice. *Blood*. 2014;123:3354-3363.
6. Denorme F, De Meyer SF. The VWF-GPIb axis in ischaemic stroke: lessons from animal models. *Thromb Haemost*. 2016;116:597-604.
7. Nichols TC, Bellinger DA, Merricks EP, et al. Porcine and canine von Willebrand factor and von Willebrand disease: hemostasis, thrombosis, and atherosclerosis studies. *Thrombosis*. 2010;2010:461238.
8. Zhou M, Wang H, Zhu J, et al. Cause-specific mortality for 240 causes in China during 1990–2013: a systematic subnational analysis for the Global Burden of Disease Study 2013. *Lancet*. 2016;387:251-272.
9. Buchtele N, Schwameis M, Gilbert JC, Schorgenhofer C, Jilma B. Targeting von Willebrand factor in ischaemic stroke: focus on clinical evidence. *Thromb Haemost*. 2018;118:959-978.
10. Spiel AO, Gilbert JC, Jilma B. von Willebrand factor in cardiovascular disease: focus on acute coronary syndromes. *Circulation*. 2008;117:1449-1459.
11. Sonneveld MA, de Maat MP, Leebeek FW. von Willebrand factor and ADAMTS13 in arterial thrombosis: a systematic review and meta-analysis. *Blood Rev*. 2014;28:167-178.
12. De Meyer SF, Stoll G, Wagner DD, Kleinschnitz C. von Willebrand factor: an emerging target in stroke therapy. *Stroke*. 2012;43:599-606.
13. Knoebl P, Cataland S, Peyvandi F, et al. Efficacy and safety of open-label caplacizumab in patients with exacerbations of acquired thrombotic thrombocytopenic purpura in the HERCULES study. *J Thromb Haemost*. 2020;18(2):479-484.
14. Peyvandi F, Scully M, Kremer Hovinga JA, et al. Caplacizumab reduces the frequency of major thromboembolic events, exacerbations and death in patients with acquired thrombotic thrombocytopenic purpura. *J Thromb Haemost*. 2017;15:1448-1452.
15. Kremer Hovinga JA, Coppo P, Lämmle B, Moake JL, Miyata T, Vanhoorelbeke K. Thrombotic thrombocytopenic purpura. *Nat Rev Dis Primers*. 2017;3:17020.
16. Hawkins BM, Abu-Fadel M, Vesely SK, George JN. Clinical cardiac involvement in thrombotic thrombocytopenic purpura: a systematic review. *Transfusion*. 2008;48:382-392.
17. Hasper D, Schrage D, Niesporek S, Knollmann F, Barckow D, Oppert M. Extensive coronary thrombosis in thrombotic-thrombocytopenic purpura. *Int J Cardiol*. 2006;106:407-409.
18. Jilma-Stohlawetz P, Gorczyca ME, Jilma B, Siller-Matula J, Gilbert JC, Knobl P. Inhibition of von Willebrand factor by ARC1779 in patients with acute thrombotic thrombocytopenic purpura. *Thromb Haemost*. 2011;105:545-552.
19. Siller-Matula JM, Merhi Y, Tanguay J-F, et al. ARC15105 is a potent antagonist of von Willebrand factor mediated platelet activation and adhesion. *Arterioscler Thromb Vasc Biol*. 2012;32:902-909.
20. Huang RH, Fremont DH, Diener JL, Schaub RG, Sadler JE. A structural explanation for the antithrombotic activity of ARC1172, a DNA aptamer that binds von Willebrand factor domain A1. *Structure*. 2009;17:1476-1484.
21. Goodall AH, Jarvis J, Chand S, et al. An immunoradiometric assay for human factor VIII/von Willebrand factor (VIII:vWF) using a monoclonal antibody that defines a functional epitope. *Br J Haematol*. 1985;59:565-577.
22. Murdock PJ, Woodhams BJ, Matthews KB, Pasi KJ, Goodall AH. von Willebrand factor activity detected in a monoclonal antibody-based ELISA: an alternative to the ristocetin cofactor platelet agglutination assay for diagnostic use. *Thromb Haemost*. 1997;78:1272-1277.
23. Vangenechten I, Mayger K, Smejkal P, et al. A comparative analysis of different automated von Willebrand factor glycoprotein Ib-binding activity assays in well typed von Willebrand disease patients. *J Thromb Haemost*. 2018;16:1268-1277.
24. Jilma B, Paulinska P, Jilma-Stohlawetz P, Gilbert JC, Hutabarat R, Knobl P. A randomised pilot trial of the anti-von Willebrand factor aptamer ARC1779 in patients with type 2b von Willebrand disease. *Thromb Haemost*. 2010;104:563-570.

25. Folts J. An in vivo model of experimental arterial stenosis, intimal damage, and periodic thrombosis. *Circulation*. 1991;83:IV3-14.
26. Firbas C, Siller-Matula JM, Jilma B. Targeting von Willebrand factor and platelet glycoprotein Ib receptor. *Expert Rev Cardiovasc Ther*. 2010;8:1689-1701.
27. Catto AJ, Carter AM, Barrett JH, Bamford J, Rice PJ, von Grant PJ. Willebrand factor and factor VIII: C in acute cerebrovascular disease. relationship to stroke subtype and mortality. *Thromb Haemost*. 1997;77:1104-1108.
28. Sanders YV, Eikenboom J, de Wee EM, et al. Reduced prevalence of arterial thrombosis in von Willebrand disease. *J Thromb Haemost*. 2013;11:845-854.
29. Seaman CD, Yabes J, Comer DM, Ragni MV. Does deficiency of von Willebrand factor protect against cardiovascular disease? Analysis of a national discharge register. *J Thromb Haemost*. 2015;13:1999-2003.
30. Douglas A, Fitzgerald S, Mereuta OM, et al. Platelet-rich emboli are associated with von Willebrand factor levels and have poorer revascularization outcomes. *J Neurointerv Surg*. 2019. https://doi.org/10.1136/neurintsurg-2019-015410
31. Sambola A, Del Blanco B, Ruiz-Meana M, et al. Increased von Willebrand factor, P-selectin and fibrin content in occlusive thrombus resistant to lytic therapy. *Thromb Haemost*. 2016;115:1129-1137.
32. Gardiner EE, Andrews RK. Structure and function of platelet receptors initiating blood clotting. *Adv Exp Med Biol*. 2014;844:263-275.
33. De Meyer SF, Schwarz T, Deckmyn H, et al. Binding of von Willebrand factor to collagen and glycoprotein Ibalpha, but not to glycoprotein IIb/IIIa, contributes to ischemic stroke in mice–brief report. *Arterioscler Thromb Vasc Biol*. 2010;30:1949-1951.
34. Kovacevic KD, Gilbert JC, Jilma B. Pharmacokinetics, pharmacodynamics and safety of aptamers. *Adv Drug Deliv Rev*. 2018;134:36-50.
35. Diener JL, Daniel lagassé HA, Duerschmied D, et al. Inhibition of von Willebrand factor-mediated platelet activation and thrombosis by the anti-von Willebrand factor A1-domain aptamer ARC1779. *J Thromb Haemost*. 2009;7:1155-1162.
36. Markus HS, McCollum C, Imray C, Goulder MA, Gilbert J, King A. The von Willebrand inhibitor ARC1779 reduces cerebral embolization after carotid endarterectomy: a randomized trial. *Stroke*. 2011;42:2149-2153.
37. Cataland SR, Peyvandi F, Mannucci PM, et al. Initial experience from a double-blind, placebo-controlled, clinical outcome study of ARC1779 in patients with thrombotic thrombocytopenic purpura. *Am J Hematol*. 2012;87:430-432.
38. Jilma-Stohlawetz P, Knobl P, Gilbert JC, Jilma B. The anti-von Willebrand factor aptamer ARC1779 increases von Willebrand factor levels and platelet counts in patients with type 2B von Willebrand disease. *Thromb Haemost*. 2012;108:284-290.
39. Jilma-Stohlawetz P, Gilbert JC, Gorczyca ME, Knobl P, Jilma B. A dose ranging phase I/II trial of the von Willebrand factor inhibiting aptamer ARC1779 in patients with congenital thrombotic thrombocytopenic purpura. *Thromb Haemost*. 2011;106:539-547.
40. Stidl R, Fuchs S, Bossard M, Siekmann J, Turecek PL, Putz M. Safety of PEGylated recombinant human full-length coagulation factor VIII (BAX 855) in the overall context of PEG and PEG conjugates. *Haemophilia*. 2016;22:54-64.
41. Ulrichts H, Silence K, Schoolmeester A, et al. Antithrombotic drug candidate ALX-0081 shows superior preclinical efficacy and safety compared with currently marketed antiplatelet drugs. *Blood*. 2011;118:757-765.
42. Sargentini-Maier ML, De Decker P, Tersteeg C, Canvin J, Callewaert F, De Winter H. Clinical pharmacology of caplacizumab for the treatment of patients with acquired thrombotic thrombocytopenic purpura. *Expert Rev Clin Pharmacol*. 2019;12:537-545.
43. Siller-Matula JM, Plasenzotti R, Spiel A, Quehenberger P, Jilma B. Interspecies differences in coagulation profile. *Thromb Haemost*. 2008;100:397-404.
44. Braeuninger S, Kleinschnitz C. Rodent models of focal cerebral ischemia: procedural pitfalls and translational problems. *Exp Transl Stroke Med*. 2009;1:8.
45. Verhenne S, Denorme F, Libbrecht S, et al. Platelet-derived VWF is not essential for normal thrombosis and hemostasis but fosters ischemic stroke injury in mice. *Blood*. 2015;126:1715-1722.
46. Derhaschnig U, Pachinger C, Jilma B. Variable inhibition of high-shear-induced platelet plug formation by eptifibatide and tirofiban under conditions of platelet activation and high von Willebrand release: a randomized, placebo-controlled, clinical trial. *Am Heart J*. 2004;147:E17.
47. Spiel AO, Derhaschnig U, Schwameis M, Bartko J, Siller-Matula JM, Jilma B. Effects of prasugrel on platelet inhibition during systemic endotoxaemia: a randomized controlled trial. *Clin Sci (Lond)*. 2012;123:591-600.
48. King A, Markus HS. Doppler embolic signals in cerebrovascular disease and prediction of stroke risk: a systematic review and meta-analysis. *Stroke*. 2009;40:3711-3717.
49. de Borst GJ, Hilgevoord A, de Vries J, et al. Influence of antiplatelet therapy on cerebral micro-emboli after carotid endarterectomy using postoperative transcranial Doppler monitoring. *Eur J Vasc Endovasc Surg*. 2007;34:135-142.
50. J. Evan Sadler III MD PhD (9 November 1951–13 December 2018). *J Thromb Haemost*. 2019;17:420-421.

## SUPPORTING INFORMATION

Additional supporting information may be found online in the Supporting Information section.

**How to cite this article:** Zhu S, Gilbert JC, Hatala P, et al. The development and characterization of a long acting anti-thrombotic von Willebrand factor (VWF) aptamer. *J Thromb Haemost*. 2020;18:1113–1123. https://doi.org/10.1111/jth.14755